Microscopic theory of the intracollisional field effect in semiconductor superlattices

Microscopic theory of the intracollisional field effect in semiconductor superlattices

Jörg Hader, Torsten Meier,* and Stephan W. Koch
Fachbereich Physik und Zentrum für Materialwissenschaften, Philipps-Universität Marburg, Renthof 5, D-35032 Marburg, Germany

Fausto Rossi
Instituto Nazionale Fisica della Materia (INFM), and Dipartimento di Fisica, Università di Modena, Via Campi 213/A, I-41100 Modena, Italy

Norbert Linder
Institut für Technische Physik I, Friedrich-Alexander-Universität Erlangen-Nürnberg, Erwin-Rommel Straβe 1, D-91058 Erlangen, Germany

(Received 29 August 1996; revised manuscript received 6 February 1997)

A detailed analysis of the optical and transport properties of semiconductor superlattices in the high-field regime is presented. Electronic Bloch oscillations and the resulting terahertz emission signals are computed including phonon damping in the presence of the electric field. The modifications of the phonon-induced terahertz signal decay are analyzed including the movement of the carriers in the field (intracollisional field effect). For elevated fields it is shown that the interplay between electric field and electron-phonon interaction leads to resonance structures in the terahertz damping rate. [S0163-1829(97)05620-8]

I. INTRODUCTION

Since the early 1990s several groups succeeded in calculating linear absorption spectra of semiconductor superlattices (SSL's) with applied electric fields, taking into account the fully three-dimensional Coulomb problem. Different approaches have been applied, each of which presents certain advantages in studying distinct aspects of the problem. Linder *et al.*,[1,2] starting from the single-particle eigenstates of the problem [i.e., Wannier-Stark (WS) states along the growth and field direction, multiplied by two-dimensional plane waves (PW's)], proposed a direct diagonalization of the superlattice Hamiltonian including Coulomb interaction within the Hartree-Fock approximation. This method allows for a detailed study of the contribution of specific states to the absorption spectrum, which is important to investigate, e.g., Fano resonances occurring due to the coupling of WS excitons to the continua of energetically lower lying WS transitions.

Following a different approach, Whittaker[3] proposed a calculation of the absorption spectrum based on a real-space description. This leads to a differential equation that can be integrated numerically. The advantage of this method is that one can focus on an arbitrarily small region of the spectrum, thus avoiding any numerical restrictions to the energy resolution.

Both methods are clearly limited to the analysis of static electric fields. In order to analyze the coherent and incoherent ultrafast phenomena in dynamically driven SSL's, Meier *et al.*[4] and Rossi *et al.*[5] used the well-known semiconductor Bloch equations[6–8] (SBE's). With this approach they successfully studied not only linear and nonlinear absorption in superlattice systems, but also the influence of carrier-phonon scattering on Bloch oscillations and terahertz (THz) radiation. Expanding the electron-hole states in terms of three-dimensional PW's it is also possible to investigate the influence of time-dependent fields. However, at the level of the commonly employed Markov approximation, one ignores the drift in k space induced by the external field during the collision, i.e., the intracollisional field effect (ICFE). Non-Markovian calculations[9,10] are possible in principle, but quite impracticable due to their high demands on computer time.

In order to investigate the significance and the characteristic features of the ICFE in SSL's we compare the results of two approaches that yield equivalent results for the full low-field dynamics and for the coherent dynamics at all field strengths. In one approach we develop the SBE's in terms of WS states, thus implicitly taking into account the dominant contribution to the ICFE (Refs. 11 and 12) (except for small corrections due to the Coulomb interaction) since WS states are eigenstates of the problem including the field. We compare these results to calculations using eigenstates of the superlattice without field, i.e., superlattice Bloch states, which neglect the ICFE completely. This comparison allows us to extract the main features of the ICFE.

Whereas the ICFE is known to have only a small influence on the relaxation behavior in bulk semiconductors, our analysis shows that it dramatically changes the electron-phonon interaction in the high-field regime of SSL's. The discrete spectrum of the WS states leads to sharp resonances in the electron-phonon scattering rates for fields where the phonon energy is a multiple integer of the WS energy splitting. Especially the parameter regions without resonances (i.e., weak damping) could be highly interesting for the possible use of SSL's as tunable emitters of THz radiation.[13]

This paper is organized as follows: In Sec. II we develop the SBE's including electron-phonon scattering in the WS and PW representations and verify that both approaches yield equivalent results for the coherent dynamics. After a brief discussion of our numerical solution procedure (Sec.

III), we present in Sec. IV linear-absorption results and analyze the influence of the electron-phonon interaction on computed THz spectra. Our results are summarized in Sec. V.

II. THEORETICAL APPROACH

The total Hamiltonian $\mathbf{H}$ for our model system, i.e., an infinite SSL with a static and homogeneous electric field $\mathbf{F}$ applied along the growth direction z, can be arranged as the sum of two terms:

$$\mathbf{H}=\mathbf{H}_1+\mathbf{H}_2\,, \tag{1}$$

where $\mathbf{H}_1$ describes the bare carrier system and its interaction with the light, and $\mathbf{H}_2$ contains the phonon contributions:

$$\mathbf{H}_1=\mathbf{H}_\mathbf{F}+\mathbf{H}_{\mathrm{Coul}}+\mathbf{H}_{\mathrm{cl}}\,, \tag{2}$$

where

$$\mathbf{H}_\mathbf{F}=\mathbf{H}_\mathbf{F}^e+\mathbf{H}_\mathbf{F}^h=[\mathbf{H}_\mathbf{0}^e+e\mathbf{F}\cdot\mathbf{r}_e]+[\mathbf{H}_\mathbf{0}^h-e\mathbf{F}\cdot\mathbf{r}_h]$$

$$=\sum_{i,i'} a^e_{i,i'}c_i^\dagger c_{i'}+\sum_{j,j'} a^h_{j,j'}d_j^\dagger d_{j'} \tag{3}$$

is the single-particle Hamiltonian for carriers in a SSL with an applied electric field $\mathbf{F}$. $\mathbf{H}_\mathbf{0}^{e(h)}$ is the Hamiltonian of a single electron (hole) in the unperturbed superlattice. c_i ($c_i^\dagger$) and d_j ($d_j^\dagger$) are the annihilation (creation) operators of electrons and holes with quantum numbers i and j. The quantities $a^e_{i,i'}$ ($a^h_{j,j'}$) denote the matrix elements of $\mathbf{H}_\mathbf{F}^{e(h)}$ in a generic electron (hole) basis $[\Psi_i^e(\mathbf{r}_e)]$ ($[\Psi_j^h(\mathbf{r}_h)\}]$. $\mathbf{H}_{\mathrm{Coul}}$ describes the Coulomb interaction for which we apply the monopole-monopole approximation.[14,15] Since we will investigate the regime of relatively low electron and hole densities (low-excitation regime), we assume an unscreened Coulomb potential. The dipole interaction of the carrier system with a classical light field, $\mathbf{H}_{\mathrm{cl}}$, is treated in a rotating-wave approximation.[5]

The phononic part of the Hamiltonian can be written as

$$\mathbf{H}_2=\mathbf{H}_p+\mathbf{H}_{\mathrm{cp}}\,. \tag{4}$$

The free-phonon dynamics is described by $\mathbf{H}_p=\Sigma_\mathbf{q}\hbar\omega_\mathbf{q}b_\mathbf{q}^\dagger b_\mathbf{q}$, where $b_\mathbf{q}^\dagger$ ($b_\mathbf{q}$) are the creation (annihilation) operators of a phonon with wave vector $\mathbf{q}$ and $\omega_\mathbf{q}$ is the corresponding phonon dispersion. For simplicity, we consider a single dispersionless bulk LO-phonon branch only ($\omega_\mathbf{q}=\omega_0\,,\forall\mathbf{q}$). Previous investigations[5,16,17] have shown that the total electron-phonon scattering rates in SSL's with similar dielectric constants in wells and barriers such as, e.g., in the GaAs-AlAs system, which we will study here, can be approximated sufficiently well using these assumptions. $\mathbf{H}_{\mathrm{cp}}$ is the carrier-phonon interaction.[5,8]

Following standard procedures[6–8,14,15,18] we now set up the equations of motions for the interband polarizations

$$Y_{ji}=\langle d_j c_i\rangle,\quad Y_{ji}^\star=\langle c_i^\dagger d_j^\dagger\rangle \tag{5}$$

and the electron and hole density-matrix elements

$$C_{ii'}=\langle c_i^\dagger c_{i'}\rangle,\quad D_{jj'}=\langle d_j^\dagger d_{j'}\rangle. \tag{6}$$

The diagonal elements of the electron (hole) density matrix give the electron (hole) occupation probabilities. Due to the loss of translational invariance, in general, the density matrices also contain off-diagonal elements. These intraband polarizations describe the coherence between different electron or hole states. The total dipole moment P is the sum of the interband part P^{inter} and the intraband part P^{intra}

$$P=P^{\mathrm{inter}}+P^{\mathrm{intra}}, \tag{7}$$

$$P^{\mathrm{inter}}=\sum_{i,j}\,[\mu_{ij}^{eh}Y_{ji}^\star-(\mu_{ij}^{eh})^\star Y_{ji}],$$

$$P^{\mathrm{intra}}=\sum_{i,i'}\,\mu_{ii'}^{ee}C_{ii'}+\sum_{j,j'}\,\mu_{jj'}^{hh}D_{jj'}, \tag{8}$$

with (interband) intraband dipole matrix elements (μ^{eh}) μ^{ee}, μ^{hh}

$$\mu_{ij}^{eh}=\mu_0\langle\Psi_i^e|\Psi_j^h\rangle,\quad \mu_{ii'}^{ee}=-e\langle\Psi_i^e|z|\Psi_{i'}^e\rangle,$$

$$\mu_{jj'}^{hh}=-e\langle\Psi_j^h|z|\Psi_{j'}^h\rangle. \tag{9}$$

The quantum numbers i and j may label any complete set of orthonormal states. In the PW approach these are eigenstates of the SSL without field $\mathbf{H}_\mathbf{0}^{e/h}(\mathbf{r}_{e/h})$, i.e., superlattice Bloch states

$$\Psi^{e/h}_{\mathbf{k}\nu/\mu}(\mathbf{r})=\frac{1}{\sqrt{A}}e^{i\mathbf{k}\cdot\mathbf{r}}f^{e/h}_{k_z\nu/\mu}(z), \tag{10}$$

with

$$\mathbf{H}_\mathbf{0}^{e/h}\Psi^{e/h}_{\mathbf{k}\nu/\mu}=\varepsilon^{e/h}_{\mathbf{k}\nu/\mu}\Psi^{e/h}_{\mathbf{k}\nu/\mu}=\left[\frac{\hbar^2k_\parallel^2}{2m_{e/h}}+\epsilon^{e/h}_{k_z\nu/\mu}\right]\Psi^{e/h}_{\mathbf{k}\nu/\mu}\,. \tag{11}$$

The z parts $f^{e/h}_{k_z\nu/\mu}(z)$ are periodic with the SSL period d. ν (μ) is the electron (hole) miniband index. We employ the Kronig-Penny model[19] to determine the superlattice Bloch functions and the miniband dispersions $\epsilon_{k_z\nu/\mu}$.

In the WS description we use PW's for the in-plane motion but for the growth and field direction we take WS states ϕ_p:

$$\Psi^{e/h}_{\mathbf{k}_\parallel p\nu/\mu}(\mathbf{r})=\frac{1}{\sqrt{A}}e^{i\mathbf{k}_\parallel\cdot\mathbf{r}_\parallel}\phi^{e/h}_{p\nu/\mu}(z), \tag{12}$$

$$\phi^{e/h}_{p\nu/\mu}(z)=\frac{d}{2\pi}\int_{-\pi/d}^{\pi/d}\exp\left[\frac{i}{eF}\int_0^{k_z}[\epsilon^{e/h}_{\nu/\mu}(k_z')-\epsilon^{e/h}_{p\nu/\mu}]dk_z'\right]e^{ik_zz}f^{e/h}_{k_z\nu/\mu}(z)dk_z\,, \tag{13}$$

with

$$\epsilon^{e/h}_{p=0,\nu/\mu}=\frac{d}{2\pi}\int_{-\pi/d}^{\pi/d}\epsilon^{e/h}_{\nu/\mu}(k_z')dk_z', \tag{14}$$

$$\epsilon^{e/h}_{p\nu/\mu}=\epsilon^{e/h}_{0\nu/\mu}+peFd, \tag{15}$$

and $p\in\{0,\pm1,\pm2,\ldots\}$. In the developement of the WS states we restrict ourselves to linear combinations of single-particle eigenstates of the field-free SSL with only one mini-

band. Thus we neglect field-induced intersubband coupling (Zener transitions), which is a reasonable approximation[20,21] for the parameters used in our study. At very high fields this coupling may become more important but, nevertheless, will not dominate the properties we want to study in this paper.

The WS states are eigenstates of $\mathbf{H}_{\mathbf{F}}^{e/h}$:

$$\mathbf{H}_{\mathbf{F}}^{e/h}\Psi_{\mathbf{k}_\parallel p\nu/\mu}^{e/h}=\varepsilon_{\mathbf{k}_\parallel p\nu/\mu}^{e/h}\Psi_{\mathbf{k}_\parallel p\nu/\mu}^{e/h}=\left[\frac{\hbar^2k_\parallel^2}{2m_{e/h}}+\epsilon_{p=0,\nu/\mu}^{e/h}+peFd\right]\Psi_{\mathbf{k}_\parallel p\nu/\mu}^{e/h}. \tag{16}$$

The states with different p are related to another by

$$\phi_{p'\nu/\mu}^{e/h}(z)=\phi_{p\nu/\mu}^{e/h}[z-(p'-p)d]. \tag{17}$$

A change from the PW to the WS representation can be achieved through the following unitary transformation:

$$\phi_{p\nu/\mu}^{e/h}(z)=\sum_{k_z}U_{k_zp\nu/\mu}^{e/h}[e^{ik_zz}f_{k_z\nu/\mu}^{e/h}(z)], \tag{18}$$

$$U_{k_zp\nu/\mu}^{e/h}=\exp\left[\frac{i}{eF}\int_0^{k_z}[\epsilon_{\nu/\mu}^{e/h}(k_z')-\epsilon_{p\nu/\mu}^{e/h}]dk_z'\right]. \tag{19}$$

It is well known[22] that the limiting case $F=0$ cannot be properly described in the WS picture, as it would require an infinite set of WS eigenstates to be taken into account. Thus, also the unitary transformation is only defined for nonvanishing fields.

The explicit form of the Hamiltonian is obtained in the PW approach identifying

$$i\rightarrow(\mathbf{k},\nu),\quad j\rightarrow(-\mathbf{k},\mu), \tag{20}$$

and in the WS approach

$$i\rightarrow(\mathbf{k}_\parallel,p,\nu),\quad j\rightarrow(-\mathbf{k}_\parallel,p,\mu). \tag{21}$$

The matrix elements of $\mathbf{H}_{\mathbf{F}}$ in the PW representation are given by

$$a_{\mathbf{k}\nu,\mathbf{k}'\nu'}^{e}=[\varepsilon_{\mathbf{k}\nu}^{e}+ie\mathbf{F}\cdot\boldsymbol{\nabla}_{\mathbf{k}}]\delta_{\mathbf{k}\mathbf{k}'}\delta_{\nu\nu'},$$
$$a_{\mathbf{k}\mu,\mathbf{k}'\mu'}^{h}=[\varepsilon_{\mathbf{k}\mu}^{h}-ie\mathbf{F}\cdot\boldsymbol{\nabla}_{\mathbf{k}}]\delta_{\mathbf{k}\mathbf{k}'}\delta_{\mu\mu'} \tag{22}$$

if, as already done for the WS states, interminiband Zener transitions are neglected. In the WS representation the matrix elements of $\mathbf{H}_{\mathbf{F}}$ are the single-particle energies $\varepsilon_{\pm\mathbf{k}_\parallel p\nu/\mu}^{e/h}$.

In the PW representation the polarizations and distribution functions only depend on the relative wave vector (if, as in our case, the momentum of the photon is neglected):

$$Y_{-\mathbf{k}\mu,\mathbf{k}'\nu}\rightarrow Y_{(\mathbf{k}'-\mathbf{k}),\mu\nu} \tag{23}$$

and similarly for C and D. The same is true for the in-plane motion in the WS representation. In the latter approach, the exclusive dependence on the relative wave vector for the growth direction leads to a dependence on the relative WS index p only

$$Y_{-\mathbf{k}_\parallel p\mu,\mathbf{k}_\parallel' p'\nu}\rightarrow Y_{(\mathbf{k}_\parallel'-\mathbf{k}_\parallel),(p'-p),\mu\nu}. \tag{24}$$

In a time-dependent Hartree-Fock approximation the equations of motion for Y, C, and D due to $\mathbf{H}_1$ are the semiconductor Bloch equations (SBE's).[8,14,15] In the WS representation, using Eqs. (21) and (24), the SBE's for a superlattice with an applied homogeneous electric field $\mathbf{F}$ are

$$\begin{aligned}\frac{d}{dt}Y_{\mathbf{k}_\parallel,p_1,\mu_1\nu_1}=&\frac{1}{i\hbar}\sum_{p_2,\nu_2,\mu_2}[\mathcal{E}^{e}_{\mathbf{k}_\parallel,p_2-p_1,p_1+p',\nu_1\nu_2}\delta_{\mu_1\mu_2}\\&+\mathcal{E}^{h}_{\mathbf{k}_\parallel,p_1-p_2,-p',\mu_1\mu_2}\delta_{\nu_1\nu_2}]Y_{\mathbf{k}_\parallel,p_2,\mu_2\nu_2}\\&-\frac{1}{i\hbar}\sum_{p_2,\nu_2,\mu_2}\mathcal{U}_{\mathbf{k}_\parallel,p_1-p_2,\nu_2\mu_2}\\&\times[C_{\mathbf{k}_\parallel,p_2,\nu_2\nu_1}\delta_{\mu_1\mu_2}+D_{-\mathbf{k}_\parallel,-p_2,\mu_2\mu_1}\delta_{\nu_1\nu_2}\\&-\delta_{\nu_1\nu_2}\delta_{\mu_1\mu_2}\delta_{p_1,p_2}],\end{aligned} \tag{25}$$

$$\begin{aligned}\frac{d}{dt}C_{\mathbf{k}_\parallel,p_1,\nu_1\nu_2}=&\frac{1}{i\hbar}\sum_{p_2,\nu_3,\nu_4}[\mathcal{E}^{e}_{\mathbf{k}_\parallel,p_1-p_2,p_1+p'\nu_2\nu_4}\delta_{\nu_1\nu_3}\\&-\mathcal{E}^{e}_{\mathbf{k}_\parallel,p_1-p_2,p'\nu_3\nu_1}\delta_{\nu_2\nu_4}]C_{\mathbf{k}_\parallel,p_2,\nu_3\nu_4}\\&+\frac{1}{i\hbar}\sum_{p_2,\mu_1}[\mathcal{U}_{\mathbf{k}_\parallel,p_1-p_2,\nu_2\mu_1}Y^{\star}_{\mathbf{k}_\parallel,-p_2,\mu_1\nu_1}\\&-\mathcal{U}^{\star}_{\mathbf{k}_\parallel,p_1-p_2,\nu_1\mu_1}Y_{\mathbf{k}_\parallel,p_2,\mu_1\nu_2}],\end{aligned} \tag{26}$$

$$\begin{aligned}\frac{d}{dt}D_{-\mathbf{k}_\parallel,p_1,\mu_1\mu_2}=&\frac{1}{i\hbar}\sum_{p_2,\nu_3,\nu_4}[\mathcal{E}^{h}_{\mathbf{k}_\parallel,p_1-p_2,p_1+p'\mu_2\mu_4}\delta_{\mu_1\mu_3}\\&-\mathcal{E}^{h}_{\mathbf{k}_\parallel,p_1-p_2,p'\mu_3\mu_1}\delta_{\mu_2\mu_4}]D_{-\mathbf{k}_\parallel,p_2,\mu_3\mu_4}\\&+\frac{1}{i\hbar}\sum_{p_2,\mu_1}[\mathcal{U}_{\mathbf{k}_\parallel,p_2-p_1,\nu_1\mu_2}Y^{\star}_{\mathbf{k}_\parallel,p_2,\mu_1\nu_1}\\&-\mathcal{U}^{\star}_{\mathbf{k}_\parallel,p_2-p_1,\nu_1\mu_1}Y_{\mathbf{k}_\parallel,-p_2,\mu_2\nu_1}],\end{aligned} \tag{27}$$

with

$$\begin{aligned}\mathcal{E}^{e}_{\mathbf{k}_\parallel,p_1,p_2,\nu_1\nu_2}&=\varepsilon^{e}_{\mathbf{k}_\parallel,p_2,\nu_1}\delta_{p_1}\delta_{\nu_1\nu_2}+\hbar\Omega^{e}_{\mathbf{k}_\parallel,p_1,\nu_1\nu_2}\\&=\varepsilon^{e}_{\mathbf{k}_\parallel,p_2,\nu_1}\delta_{p_1}\delta_{\nu_1\nu_2}-\sum_{\mathbf{k}_\parallel',p_3,\nu_3,\nu_4}\\&\times V^{p_3,p_1}_{\nu_3\nu_4\nu_2\nu_1}(\mathbf{k}_\parallel-\mathbf{k}_\parallel')\\&\times C_{\mathbf{k}_\parallel',p_3,\nu_3\nu_4},\end{aligned} \tag{28}$$

$$\begin{aligned}\mathcal{E}^{h}_{\mathbf{k}_\parallel,p_1,p_2,\mu_1\mu_2}&=\varepsilon^{h}_{\mathbf{k}_\parallel,p_2,\nu_1}\delta_{p_1}\delta_{\mu_1\mu_2}+\hbar\Omega^{h}_{\mathbf{k}_\parallel,p_1,\mu_1\mu_2}\\&=\varepsilon^{h}_{\mathbf{k}_\parallel,p_2,\mu_1}\delta_{p_1}\delta_{\mu_1\mu_2}-\sum_{\mathbf{k}_\parallel',p_3\mu_3,\mu_4}\\&\times V^{p_3,p_1}_{\mu_3\mu_4\mu_2\mu_1}(\mathbf{k}_\parallel-\mathbf{k}_\parallel')\\&\times D_{\mathbf{k}_\parallel',p_3,\mu_3\mu_4},\end{aligned} \tag{29}$$

$$\mathcal{U}_{\mathbf{k}_\parallel,p_1,\nu_1\mu_1} = -\mu^{eh}_{p_1,\nu_1\mu_1}E^+(t)+\Delta_{\mathbf{k}_\parallel,\nu_1\mu_1}$$
$$= -\mu^{eh}_{p_1,\nu_1\mu_1}E^+(t)-\sum_{\mathbf{k}'_\parallel,p_2,\nu_2,\mu_2} V^{p_2,p_1}_{\mu_1\nu_1\mu_2\nu_2} \times(\mathbf{k}_\parallel-\mathbf{k}'_\parallel)Y_{\mathbf{k}'_\parallel,p_2,\mu_2\nu_2}. \quad (30)$$

Here we have assumed $\mathbf{k}_\parallel$-independent dipole matrix elements μ^{eh}. $\hbar\Omega^{e(h)}$ is the self-energy matrix due to the electron-electron (hole-hole) interaction, Δ is the internal-field matrix due to electron-hole interaction, and $\mathcal{U}$ denotes the renormalized field. The Coulomb matrix elements are given by

$$V^{p_1,p_2}_{n_1n_2n_3n_4}(\mathbf{k}_\parallel-\mathbf{k}'_\parallel)=\sum_{p'_1,p'_2}\langle\Psi_{\mathbf{k}_{\parallel 1},p'_1,n_1}\Psi_{\mathbf{k}_{\parallel 2},p_1+p'_1,n_2}|V_{\mathrm{Coul}}|\Psi_{\mathbf{k}_{\parallel 3},p'_2,n_3}\Psi_{\mathbf{k}_{\parallel 4},p_2+p'_2,n_4}\rangle\cdot\delta(\mathbf{k}_\parallel-\mathbf{k}_{\parallel 1}+\mathbf{k}_{\parallel 2})\,\delta(\mathbf{k}'_\parallel-\mathbf{k}_{\parallel 3}+\mathbf{k}_{\parallel 4}). \quad (31)$$

The corresponding equations in the PW representation are obtained from Eqs. (25)–(30) by deleting all dependencies on p, changing from $\mathbf{k}_\parallel$ to $\mathbf{k}$, and replacing $\varepsilon^{(e/h)}$ by the matrix elements of $\mathbf{H_F}$, $a^{(e/h)}$ [eq. (22)]. It is worthwhile to stress at this point that the equations derived so far in the two approaches are totally equivalent and can be transformed into each other using the unitary transformation $U^{e/h}_{k_z p\nu/\mu}$.

In the next step we include the additive contributions in the dynamic equations due to the interaction between carriers and optical phonons as modeled by the term $\mathbf{H}_2$ in Eq. (1). We have verified numerically that for the relatively low excitation densities used in our calculations, it is a good approximation to ignore the carrier-carrier Coulomb scattering effects.

As usual, the phonon-interaction contributions in the equations of motion for Y, C, and D due to $\mathbf{H}_2$ lead to a hierarchy of coupled dynamic variables, which has to be broken at a certain order (in the interaction Hamiltonian). In the present analysis we do not want to consider phonon-assisted density matrices of the form $\langle c^\dagger_i b_{\mathbf{q}} c_{i'}\rangle$ as additional dynamic variables, since this would lead to extremely time consuming non-Markovian calculations. Hence, we restrict our approach to the two-particle density matrices Y, C, and D by employing the Markov approximation.[23–25]

The physical picture behind the Markov approximation is that one assumes the carriers to stay in their state for the duration of a scattering process. Of course, this is only true if these states are eigenstates of $\mathbf{H}$. In particular, here, due to the field the carriers move through the mini-Brillouin zone. If one develops the problem in terms of PW's, the carriers are described as moving from one $\Psi_{\mathbf{k}_\parallel,k_z}$ to another $\Psi_{\mathbf{k}_\parallel,k_{z'}}$. This transition rate increases with increasing field. Therefore, for higher fields this approach becomes less and less appropriate. However, the WS picture implicitly accounts for this intracollisional field effect (at least on the single-particle level) since the WS states are single-particle eigenstates of the Hamiltonian $\mathbf{H_F}$. These eigenstates include the electric field and, therefore, the WS approach is expected to better account for the electron-phonon relaxation process in the high-field regime.

Evaluating the equations of motion and applying the Markov approximation in the WS representation we obtain

$$\frac{d}{dt}C_{\mathbf{k}_\parallel,p_1,\nu_1\nu_2}\Big|_{\mathbf{H}_2}=\frac{\pi}{\hbar}\sum_{\mathbf{k}'_\parallel,p_2,\nu_3,\mathbf{q}}\Bigg\{g^{e,\nu_3\nu_1}_{\mathbf{k}'_\parallel,\mathbf{k}_\parallel,p_2,\mathbf{q}}\Bigg[\sum_{p_3,\nu_4}[\tilde{g}^{e,\nu_2\nu_4\star}_{\mathbf{k}_\parallel,\mathbf{k}'_\parallel,p_3,-p_1-p_3,\mathbf{q}}\mathcal{D}(\omega^{ee-}_{\mathbf{k}_\parallel,\mathbf{k}'_\parallel,p_3,\nu_2,\nu_4,\mathbf{q}})C_{\mathbf{k}'_\parallel,p_1+p_2+p_3,\nu_3\nu_4}n_{\mathbf{q}}$$
$$-\tilde{g}^{e,\nu_4\nu_3\star}_{\mathbf{k}_\parallel,\mathbf{k}'_\parallel,p_3,p_1,\mathbf{q}}\mathcal{D}(\omega^{ee-}_{\mathbf{k}_\parallel,\mathbf{k}'_\parallel,p_3,\nu_4,\nu_3,\mathbf{q}})C_{\mathbf{k}_\parallel,p_1+p_2+p_3,\nu_4\nu_2}(1+n_{\mathbf{q}})]$$
$$+\sum_{p_3,p_4,\nu_4,\nu_5}\tilde{g}^{e,\nu_4\nu_5\star}_{\mathbf{k}_\parallel,\mathbf{k}'_\parallel,p_3,p_2-p_4,\mathbf{q}}\mathcal{D}(\omega^{ee-}_{\mathbf{k}_\parallel,\mathbf{k}'_\parallel,p_3,\nu_4,\nu_5,\mathbf{q}})C_{\mathbf{k}_\parallel,p_1+p_2+p_3-p_4,\nu_4\nu_2}C_{\mathbf{k}'_\parallel,p_4,\nu_3\nu_5}$$
$$+\sum_{p_3,p_4,\mu_1,\mu_2}\tilde{g}^{h,\mu_1\mu_2\star}_{\mathbf{k}'_\parallel,\mathbf{k}_\parallel,p_3,p_2-p_4,\mathbf{q}}\mathcal{D}(\omega^{hh-}_{\mathbf{k}'_\parallel,\mathbf{k}_\parallel,p_3,\mu_1,\mu_2,\mathbf{q}})Y^\star_{\mathbf{k}'_\parallel,-p_1-p_2+p_3+p_4,\mu_1\nu_3}Y_{\mathbf{k}_\parallel,p_4,\mu_2\nu_2}\Bigg]$$
$$-g^{e,\nu_2\nu_3}_{\mathbf{k}_\parallel,\mathbf{k}'_\parallel,p_2,\mathbf{q}}\Bigg[\sum_{p_3,\nu_4}[\tilde{g}^{e,\nu_3\nu_4\star}_{\mathbf{k}'_\parallel,\mathbf{k}_\parallel,p_3,-p_3,\mathbf{q}}\mathcal{D}(\omega^{ee-}_{\mathbf{k}'_\parallel,\mathbf{k}_\parallel,p_3,\nu_3,\nu_4,\mathbf{q}})C_{\mathbf{k}_\parallel,p_1+p_2+p_3,\nu_1\nu_4}n_{\mathbf{q}}$$
$$+\tilde{g}^{e,\nu_4\nu_1\star}_{\mathbf{k}'_\parallel,\mathbf{k}_\parallel,p_3,p_2+p_1,\mathbf{q}}\mathcal{D}(\omega^{ee-}_{\mathbf{k}'_\parallel,\mathbf{k}_\parallel,p_3,\nu_4,\nu_1,\mathbf{q}})C_{\mathbf{k}'_\parallel,p_1+p_2+p_3,\nu_4\nu_3}(1+n_{\mathbf{q}})]$$
$$-\sum_{p_3,p_4,\nu_4,\nu_5}\tilde{g}^{e,\nu_4\nu_5\star}_{\mathbf{k}'_\parallel,\mathbf{k}_\parallel,p_3,p_1+p_2-p_4,\mathbf{q}}\mathcal{D}(\omega^{ee-}_{\mathbf{k}'_\parallel,\mathbf{k}_\parallel,p_3,\nu_4,\nu_5,\mathbf{q}})C_{\mathbf{k}'_\parallel,p_1+p_2+p_3-p_4,\nu_4\nu_3}C_{\mathbf{k}_\parallel,p_4,\nu_1\nu_5}$$
$$+\sum_{p_3,p_4,\mu_1,\mu_2}\tilde{g}^{h,\mu_1\mu_2\star}_{\mathbf{k}_\parallel,\mathbf{k}'_\parallel,p_3,p_1+p_2-p_4,\mathbf{q}}\mathcal{D}(\omega^{hh-}_{\mathbf{k}_\parallel,\mathbf{k}'_\parallel,p_3,\mu_1,\mu_2,\mathbf{q}})Y^\star_{\mathbf{k}_\parallel,-p_1-p_2+p_3+p_4,\mu_1\nu_1}Y_{\mathbf{k}'_\parallel,p_4,\mu_2\nu_3}\Bigg]\Bigg\}$$
$$+\{g\leftrightarrow g^\star,\tilde{g}_{p,p'}\leftrightarrow\tilde{g}^\star_{p,-p'},\omega^-\leftrightarrow\omega^+,n\leftrightarrow(n+1),CC\leftrightarrow-CC,Y^*Y\leftrightarrow-Y^*Y\}, \quad (32)$$

and similar expressions for D and Y. Here, $n_{\mathbf{q}}=\langle b_{\mathbf{q}}^{\dagger}b_{\mathbf{q}}\rangle$ denotes the phonon occupation number. Hot-phonon effects are neglected assuming that the phonon system is always in thermal equilibrium. This approximation is justified since we consider only the low excitation limit. We used

$$\begin{aligned}\hbar\omega^{ee\pm}_{\mathbf{k}_\parallel,\mathbf{k}'_\parallel,p,\nu_1,\nu_2,\mathbf{q}}&=\varepsilon^{e}_{\mathbf{k}_\parallel,p',\nu_1}-\varepsilon^{e}_{\mathbf{k}'_\parallel,p+p',\nu_2}\pm\hbar\omega_{\mathbf{q}}\\&=\frac{\hbar^2}{2m_e}(\mathbf{k}_\parallel^2-\mathbf{k}_\parallel'^2)-peFd+\epsilon^{e}_{p=0,\nu_1}\\&\quad-\epsilon^{e}_{p=0,\nu_2}\pm\hbar\omega_{\mathbf{q}},\\ \hbar\omega^{hh\pm}_{\mathbf{k}_\parallel,\mathbf{k}'_\parallel,p,\mu_1,\mu_2,\mathbf{q}}&=\varepsilon^{h}_{\mathbf{k}_\parallel,p',\mu_1}-\varepsilon^{h}_{\mathbf{k}'_\parallel,p+p',\mu_2}\pm\hbar\omega_{\mathbf{q}}\\&=\frac{\hbar^2}{2m_h}(\mathbf{k}_\parallel^2-\mathbf{k}_\parallel'^2)-peFd+\epsilon^{h}_{p=0,\mu_1}\\&\quad-\epsilon^{h}_{p=0,\mu_2}\pm\hbar\omega_{\mathbf{q}},\end{aligned}\tag{33}$$

$$\mathcal{D}(\omega)A(t)=\left[-i\frac{\mathcal{P}}{\omega}+\pi\delta(\omega)\right]A(t),\tag{34}$$

where $\mathcal{P}$ denotes the principal value. By means of Eq. (17) the products of the matrix elements of the phonon electrostatic potential[5] can be written as

$$\begin{aligned}g^{e,\nu_1\nu_2}_{\mathbf{k}'_\parallel,\mathbf{k}_\parallel,p_1,\mathbf{q}}(\tilde{g}^{e,\nu_3\nu_4}_{\mathbf{k}_\parallel,\mathbf{k}'_\parallel,p_2,p_3,\mathbf{q}})^{\star}&=g_0^2(1/q^2)J_{p_1,\nu_1,\nu_2,q_z}J^{\star}_{p_2,\nu_3,\nu_4,q_z}\\&\quad\times e^{iq_zp_3d}\delta(\mathbf{k}_\parallel-\mathbf{k}'_\parallel+\mathbf{q}_\parallel),\\ J_{p_1,\nu_1,\nu_2,q_z}&=\int dz\,\phi_{p=0,\nu_1}(z+p_1d)\,\phi_{p=0,\nu_2}(z)e^{iq_zz}.\end{aligned}\tag{35}$$

g_0 is a material constant, depending on the optical and static dielectric constants of the ''effective'' superlattice medium.

The meaning of the various terms in Eq. (32) can be recognized better by looking at the coupling constants. Their miniband indices have the same dependency as would have the ''absolute'' WS indices corresponding to single creation or annihilation operators. For example, the first two lines in Eq. (32) describe processes in which the coherence between the states ν_1 and ν_2 is ''scattered'' into a coherence between the states ν_3 and ν_4 due to a phonon-induced transition from state ν_1 to ν_3 and at the same time (and with the same phonon) a transition from state ν_2 to ν_4. Lines one and three describe processes where a coherence between the states ν_1 and ν_2 is ''scattered'' into one between ν_4 and ν_2 due to two transitions, first from ν_1 to ν_3 and then from ν_3 to ν_4. The relaxation of the distribution functions is given by Eq. (32) with $p_1=0$ and $\nu_1=\nu_2$. The other terms describe the relaxation of the intraband polarizations.

It is important to stress that if one restricts the analysis to only one electron miniband the only relaxation mechanism for the total intraband polarization is provided by transitions between different WS levels. The relaxation of the in-plane momentum does not influence the total intraband polarization.

As for the SBE's (25)–(30), the expressions for the carrier-phonon contributions in the PW approach are derived from those in the WS representation by changing $\mathbf{k}_\parallel$ to $\mathbf{k}$ and deleting all dependences on p. However, due to the applied Markov approximation, a transformation with the unitary transformation $U^{e/h}_{k_z p\nu/\mu}$ is no longer possible, since it would also imply replacing $\varepsilon^{(e/h)}_{\mathbf{k}_\parallel,p}$ by the matrix elements of $\mathbf{H_F}$, $a^{(e/h)}$ [Eq. (22)] and not, as necessary here, by $\varepsilon^{(e/h)}_{\mathbf{k}}$. If one restricts oneself to the energetically lowest electron miniband and the highest hole miniband and neglects the interband polarizations one recovers the expressions given by Rossi *et al.*,[5] having the form of the standard Boltzmann scattering equations.

The observables we are interested in are the linear absorption and the THz signal. The first one is given by[8]

$$\alpha(\omega)=\frac{\omega}{nc}\mathrm{Im}\left\{\frac{P(\omega)}{VE(\omega)}\right\},\tag{36}$$

with the background refractive index n, the speed of light c, and the crystal volume V. In the WS approach we obtain the amplitude of the THz emission from

$$I_{\mathrm{THz}}(t)\propto\frac{d^2}{dt^2}P^{\mathrm{intra}}(t),\tag{37}$$

with P^{intra} (which is a real quantity) given by Eq. (8). Since the intraband polarizations $C_{\mathbf{k}_\parallel p}$, $D_{\mathbf{k}_\parallel p}$ oscillate with the transition energies $peFd$, only the coherences between different WS states ($p\neq0$) contribute, but not the carrier distributions ($p=0$). In the PW description no intraminiband polarizations occur, since these have no driving terms in the equations of motion (the matrix elements $a^{(e/h)}$ [Eq. (22)] are diagonal in $\mathbf{k}$) when, as we do, the rotating-wave and dipole approximations are used. Here, the z dynamics is accounted for by the term $ie\mathbf{F}\cdot\boldsymbol{\nabla}_{\mathbf{k}}$ [Eq. (22)]. The THz signal is evaluated from the total current J

$$I_{\mathrm{THz}}(t)\propto\frac{d}{dt}J(t),\tag{38}$$

$$J(t)=e\left[\sum_{\mathbf{k},\nu}C_{\mathbf{k}\nu\nu}v_{\mathbf{k}\nu}+\sum_{\mathbf{k},\mu}D_{\mathbf{k}\mu\mu}v_{\mathbf{k}\mu}\right],\tag{39}$$

where v is the component of the group-velocity parallel to the field.

III. NUMERICAL PROCEDURE

For the PW and WS representations we solve the SBE's by a direct-integration approach based on a time-step discretization. The incoherent contributions to the time evolutions have to be treated differently in the two representations for several reasons: since in the PW representation the incoherent part takes the form of a standard Boltzmann equation, we apply the well established Monte Carlo technique.[5] However, this method is not applicable for the type of high-field phenomena that we want to investigate in the WS representation. Here, one has to carefully include the intraband polarizations $C_{p\neq0}, D_{p\neq0}$. These terms are orders of magnitude smaller than the distributions ($p=0$) because the corresponding interband dipole matrix elements $\mu^{eh}_{p\neq0}$ between WS states (which are strongly localized by the field on dif-

ferent wells p and p') are that much smaller and therefore allow for small excitation only. Nevertheless, these intraband polarizations carry most of the z dynamics first because they are the terms that oscillate with the Bloch frequencies ($peFd/\hbar$). Second, the contribution of the distributions to the total intraband polarization, which is responsible for, e.g., the THz radiation, is suppressed because the distributions enter multiplied by the intraband dipole matrix elements $\mu_{p=0}^{ee/hh}$, which are negligible since the localized WS states are almost symmetrical.

Moreover, contributions to the dynamics of the intraband polarizations of different magnitude and frequency give rise to strong cancellations. For these reasons, we directly evaluate the incoherent contributions to the time evolution by transforming the energy-δ functions in Eq. (32) into k-δ functions and perform linear interpolations on a dense $\mathbf{k}$ grid.

In the high-field regime the WS localization strongly suppresses the z dynamics. The remaining carrier Bloch oscillations have a very small amplitude and are hardly visible within a Monte Carlo sampling. Therefore, we calculate THz spectra in the PW approach for low and intermediate fields only. On the other hand, the numerical limitation in the WS approach is given by the number of WS states that have to be considered. With decreasing field the number of WS states in the interesting energy region increases, preventing us from going to extremely low fields in this representation.

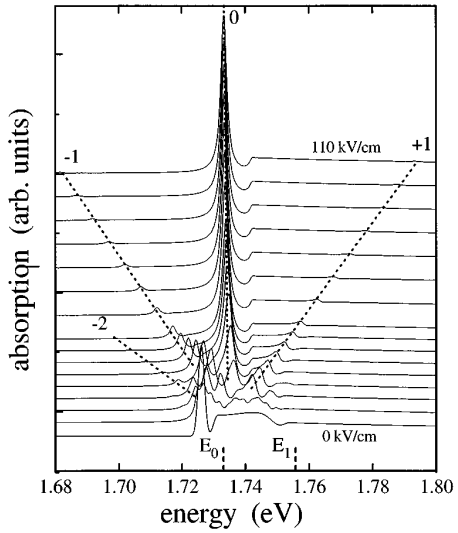

FIG. 1. Linear absorption spectra as calculated with the WS or the PW approach, for various applied electric fields. The vertical displacement between any two spectra is proportional to the difference of the corresponding fields. The WS transitions are labeled by numbers, the lower (higher) edge of the combined miniband by E_0 (E_1).

IV. APPLICATIONS

In this section we present numerical results for the case of a GaAs/AlAs superlattice structure of 34-Å well width and 17-Å barrier width. The confinement potential for the electrons (holes) is taken to be 990 meV (530 meV) and the effective electron mass in the well (barrier) material is $0.067m_0$ ($0.150m_0$). The corresponding values for the heavy holes are $0.377m_0$ ($0.508m_0$), respectively. In the perpendicular direction the effective masses are $0.0735m_0$ ($0.115m_0$) for the electrons (holes).

To simplify our discussion we consider only the lowest electron and hole miniband. With the above parameters, the resulting combined miniband has a width of $\Delta = 23$ meV. We limit ourselves to the low-excitation regime ($\mu_0 E \ll E_R$, where $E_R \approx 3.75$ meV is the three-dimensional exciton binding energy of GaAs).

As discussed above, the SBE's in the PW and WS representations are totally equivalent on the Hartree-Fock level. Therefore, both approaches provide the same linear-absorption spectra. Figure 1 shows some absorption spectra for the parameters given above. Here we used a phenomenological dephasing time T_2 of 600 fs. Theoretically, an infinite set of WS states is necessary for the unitary transformation between the two representations. Nevertheless, since only states within the miniband range or close to it have recognizable overlap and thus dipole matrix elements, only these states can be excited and carry the relevant oscillator strength. For example, polarizations with high relative WS index $|p| = |p_f - p_i|$ corresponding to $|p|eFd \gg \Delta$ are not optically active and do not influence the absorption, whether or not Coulomb interaction is taken into account. Due to the small overlap between the states with high $|p|$ these do not contribute to the transport or THz radiation too. The relation $|p|eFd \approx \Delta$ gives a good estimate about how many WS states are needed in order to get the same results as in the PW approach. For example, for 15 kV/cm we obtained an absorption line that is indistinguishable from the one in the PW approach with eleven WS states ($-5 \leq p \leq 5$). A numerically correct zero-field absorption line can be obtained in the WS approach by using a very small field, which gives a Bloch oscillation time $T_B = \hbar/eFd \ll T_2$.

Figure 1 reveals all the typical features of superlattice electroabsorption. Since the combined miniband width is larger than the two- and three-dimensional exciton Rydberg energies, it is possible to investigate the quasi-three-dimensional absorption behavior of the delocalized miniband states as well as localization effects induced by the electric field. For vanishing field one recovers the miniband absorption of the completely delocalized states. At low fields (here $\lesssim$ 10 kV/cm) the miniband Franz-Keldysh oscillations,[1] shifting with $F^{2/3}$ from the lower and higher miniband edge, E_0 and E_1, respectively, toward the center of the combined miniband, clearly modify the oscillator strength of the WS transitions. At high fields the excitonic WS ladder dominates the spectra. In the WS approach the peaks can be attributed to single-particle transitions between the states with the corresponding quantum numbers. The excitonic peak with WS index p is predominantly produced by Y_p. Therefore, the WS approach is ideally suited for a detailed study of the contributions by specific transitions. In the PW approach the WS exciton peaks cannot be associated with specific transitions, but are resonances of the total polarization.

In order to compare the incoherent dynamics within the two approaches and thus to work out the specific features of the ICFE in SSL's, we will investigate the corresponding THz signals. These are a good probe for the loss of intraband coherence in the system. Since the intraband polarizations

$C_{\mathbf{k}_\parallel p}$, $D_{\mathbf{k}_\parallel p}$ oscillate with the transition energies $peFd$, only the coherences between different WS states ($p \neq 0$) contribute in Eq. (37), but not the carrier distributions ($p=0$).

From Eqs. (37) and (38) one can see that the incoherent dynamics are treated in different ways in the two approaches. In the PW approach one considers transitions in $\mathbf{k}$ space based on the interpretation that a wave packet, created by a laser pulse, is moving through the mini-Brillouin zone. Carriers created originally at $k_z=0$ (and arbitrary $\mathbf{k}_\parallel$) are driven by the field towards $k_z=\pi/d$ where they have an additional energy corresponding to the miniband width. Then the carriers are Bragg reflected and move from $-\pi/d$ again to π/d. Without incoherent processes the electronic wave packet has the same shape after each Bloch-oscillation period $T_B=2\pi\hbar/(eFd)$. The oscillating carriers lead to an oscillating current, which results in THz radiation. Emission and absorption of phonons eventually lead to a destruction of the wave packet. The carriers become distributed more homogeneously over the mini-Brillouin zone so that the maximum current and thus the THz radiation amplitude decrease.

On the other hand, in the WS description, one does not consider moving carriers but computes the oscillating coherence between stationary states, i.e., the inter-WS-state polarizations. This coherence is destroyed if a carrier ''jumps'' due to emission or absorption of a phonon into a different WS state, which is predominantly localized in a different well. This jump is accompanied by an additional phase $\exp(iq_z pd)$ [Eq. (35)]. These phases destroy the coherence impressed by the laser pulse and lead to destructive interference of the different polarizations. As mentioned earlier, the in-plane relaxations do not disturb the total intraband polarization and thus have no influence on the THz signal.

To make the discussion as simple as possible we choose for the following numerical analysis a temperature of 10 K so that phonon absorption is negligible (phonon energy $\hbar\omega_{\mathbf{q}}=36.4$ meV). The superlattice structure is the same as in the linear absorption calculation. We assume excitation with a Gaussian pulse, $E_0(t)\propto\exp[-(t/T)^2]$, with $T=100$ fs.

For the sake of simplicity we first discuss single-particle THz signals and include the influence of the Coulomb interaction later. We start with results in the high-field regime obtained with the WS approach.

Here, the equations contain some crucial dependencies for the scattering probability: the inter-WS transitions are enhanced if the phonon energy is close to or slightly bigger than a multiple integer of the WS splitting. In this case there is no need for a transfer of high in-plane momentum $\mathbf{q}$. Since the electron-phonon coupling matrix elements g are proportional to $1/q$, Eq. (35), and these matrix elements even have to be squared in the equation for the scattering rate, Eq. (32), these resonant transitions are strongly favored. Furthermore, from energy and in-plane momentum conservation one finds that phonon emission is preferred for states close to $k_\parallel=0$ and its probability decreases as $k_\parallel^{-2}$ for large $k_\parallel$. The electron-phonon coupling constants in the WS representation are strongly field dependent. With increasing field, the WS states become more and more localized. Consequently, the coupling and the matrix elements of the phonon potential between different WS states—which are the important ones for the THz damping—become smaller. This coupling also decreases with increasing $|p_f-p_i|$.

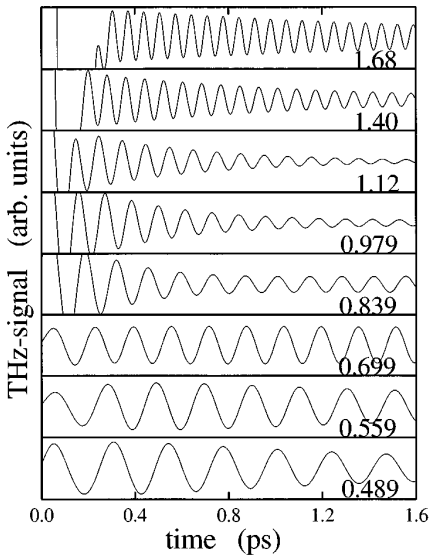

FIG. 2. THz signals for various fields obtained with the WS description. The excitation is due to a 100 fs laser pulse with a maximum at $t=0$. The laser energy was always kept on the first excited WS level ($p=1$). The numbers denote the ratio between WS splitting and phonon energy $[eFd/(\hbar\omega_0)]$.

These features are demonstrated in Fig. 2, which shows THz signals obtained with the WS approach. Here we have tuned the electric field and kept the laser energy $\hbar\omega_L$ fixed at the first excited WS level ($\hbar\omega_L=\varepsilon_1=\varepsilon_0^e+\varepsilon_0^h+eFd$). Thus, all carriers that are photoexcited into the $p=1$ level have vanishing in-plane momentum. Under these conditions the THz signal is dominated by $C_{p=\pm1}$, i.e., the coherence between two WS states predominantly located in neighboring wells whose time dependence is given by $\exp(\pm ieFd)$ (C_p is just the complex conjugate of C_{-p}, whether or not relaxation processes are taken into account). The contribution of the holes is negligible since they are almost completely localized due to their high mass even at low fields and, therefore, have very small intraband dipole matrix elements as compared to the electrons. The small overlap and thus small dipole matrix elements are also responsible for the vanishing contribution of intraband polarizations with $|p|$ higher than 1 that oscillate with p times the frequency of C_1 or D_1. Therefore, it is sufficient to look at C_1.

The emission of phonons, and thus the dephasing of these coherences, works best when the WS splitting eFd is equal to or slightly larger than the phonon energy $\hbar\omega_0$ (here, $F\gtrsim 72$ kV/cm). When the field is increased further [the ratio $eFd/(\hbar\omega_0)$ is increased] the electrons that have been excited in the p level need an increasing amount of in-plane momentum transfer to relax to the adjacent energetically lower level $(p-1)$. Thus, the corresponding coupling decreases and the dephasing of the THz signal becomes slower. This can be seen in the top three curves in Fig. 2. An exponential fit to the envelope of the THz signal leads, e.g., to a dephasing time τ of about 1.5 ps for $eFd/(\hbar\omega_0)=1.68$ and decreases to $\tau\approx 0.5$ ps for $eFd/(\hbar\omega_0)=1.12$.

When the WS splitting becomes smaller than $\hbar\omega_0$

$[1>eFd/(\hbar\omega_0)>0.5$, 72 kV/cm$>F>36$ kV/cm], the carriers have to go at least to the second nearest level, requiring a high amount of in-plane momentum transfer. The coupling between states located on wells with $|p_i-p_f|>1$ is very small for the range of fields regarded here (see Fig. 1). Therefore, there are basically no transitions between these levels and consequently almost no dephasing at all. The relaxation that can be seen in the first few hundred femtoseconds in the curves for $eFd/(\hbar\omega_0)=0.979$ and 0.839 in Fig. 2 is caused by those carriers that have been excited by the high-energy tail of the laser pulse into the $p=1$ level with sufficient in-plane momentum to be able to relax to the $p=0$ level. Since the WS states are orthogonal, the corresponding electron-phonon coupling constants have their maximum not at $q=0$ but at a small nonzero q. Therefore this initial relaxation is even faster than that at the resonant field $eFd>\approx\hbar\omega_0$.

When the field is decreased further and the WS splitting becomes equal to $0.5\hbar\omega_0$, the coupling strength increases and transitions with vanishing transfer of in-plane momentum become possible again, however, now between states with $|p_i-p_f|=2$. Therefore, the relaxation time increases again [up to $\tau\approx1.7$ ps for $eFd/(\hbar\omega_0)\approx0.5$], which is less than at the resonance at $eFd/(\hbar\omega_0)\approx1$, because the coupling between the necessary states is much smaller for the structure regarded here, even at these lower fields. Decreasing the field further, the relaxation breaks down again as it did below the first resonance.

At even lower fields, the energetic separation between resonances in the relaxation rates ($peFd=\hbar\omega_0$) decreases. Since the maximum of inter-WS coupling occurs not at $q=0$ but at a finite q, the resonances are no longer resolvable. The coupling between the states increases and becomes roughly equal for all states within the miniband. States outside the miniband region then have negligible coupling and excitation densities so that the well-known result of the PW description is recovered: a strong dependence of the relaxation on the miniband width but not on the field.[5] These results are summarized in Fig. 3, where we compare THz relaxation times as a function of the field for the WS and the PW approaches. Here we have chosen a constant excitation energy of 15 meV above the center of the combined miniband. For high fields the resonances at $eFd=0.5\hbar\omega_0$ and at $eFd=\hbar\omega_0$ are visible in the WS relaxation times again. On the other hand, the PW relaxation times are almost the same for all fields ($\tau\approx$ 550 fs) as should be expected from the continuous miniband spectrum and the electron-phonon coupling matrix elements, which are field independent in this approach. These decisive differences between the two approaches are due to the intracollisional field effect, which is neglected in the PW approach when performing the Markov approximation, whereas the WS representation implicitly accounts for most of it, at least at the level of single-particle processes. The resulting deviations become more significant with increasing field and, as demonstrated in Fig. 3, are quite dramatic in the SSL for fields in the WS localization regime. For low fields, here for $F\lesssim$ 30 kV/cm, both approaches lead to almost the same relaxation times and converge to the same zero-field result. For small fields the relaxation times in the WS approach no longer exhibit any resonances and are about 660 fs for $F=15$ kV/cm and about 780 fs for $F=25$ kV/cm.

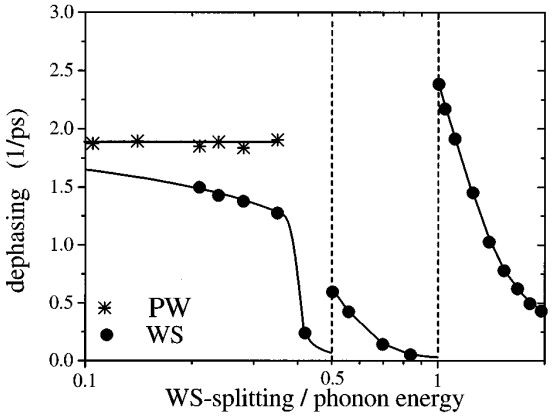

FIG. 3. Inverse decay times τ^{-1} of single-particle THz signals vs the ratio between WS splitting eFd and phonon energy $\hbar\omega_0$. The times are obtained by an exponential fit to the THz envelopes. Stars: PW approach; dots: WS description. The solid lines are a guide to the eye. The excitation energy was kept 15 meV above the center of the combined miniband.

Such a small increase of the relaxation time due to ICFE in this band-dominated regime is well known from bulk analysis.[26]

The Coulomb interaction enters the equations for the electron-phonon scattering only indirectly via its influence on Y, C, and D in the coherent part. Therefore, it has no significant influence on the relaxation of the THz signal, e.g. This is shown in Fig. 4, where we have plotted relaxation times in the WS approach as in Fig. 3, now comparing results with and without Coulomb interaction. The resonances still occur at the same ratios of WS splitting to phonon energy and are as pronounced as before.

V. CONCLUSIONS

In conclusion, we have presented a microscopic theory for the coherent and incoherent dynamics due to electron-

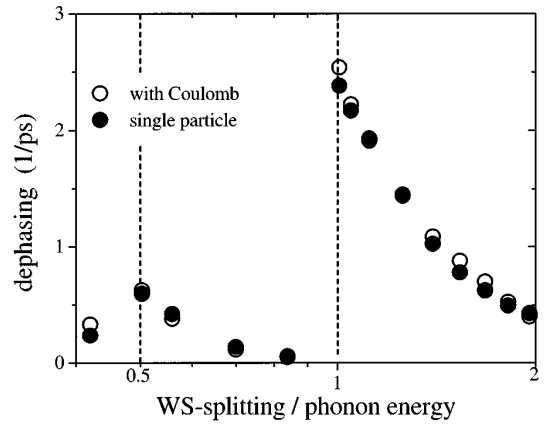

FIG. 4. Comparison between THz relaxation times in the WS approach with and without Coulomb interaction. The notation and excitation conditions are the same as in Fig. 3. Open circles: with Coulomb interaction, full circles: without Coulomb interaction.

phonon interaction of SSL's in a homogeneous electric field. We expanded the equations of motion in terms of WS states and compared the results to the more traditional PW description. Even though both approaches are totally equivalent on the Hartree-Fock level, they lead to quite substantial differences for the incoherent dynamics at high fields. These differences can be attributed to the intracollisional field effect. Most of the influence of ICFE, which has to be neglected completely in the usual PW analysis, has been taken into account implicitly in the WS representation. The comparison between the results of both approaches reveals dramatic changes in the field dependence of the relaxation of the THz radiation. For certain fields, where the phonon energy is a multiple integer of the WS splitting, the relaxation is enhanced, while for fields below these critical values relaxation is almost totally prevented. In contrast, the PW description leads to almost constant relaxation rates for all fields.

ACKNOWLEDGMENTS

This work was supported by the Deutsche Forschungsgemeinschaft through the Sonderforschungsbereich 383. T. M. presently receives financial support from the scientific branch of the NATO through the Deutscher Akademischer Austauschdienst (DAAD).

*Present address: Department of Chemistry, University of Rochester, Rochester, NY 14627.

[1] N. Linder, K. H. Schmidt, W. Geiβelbrecht, G. H. Döhler, H. T. Grahn, K. Ploog, and H. Schneider, Phys. Rev. **B 52**, 17 352 (1995).

[2] N. Linder, W. Geiβelbrecht, G. Philipp, K. H. Schmidt, and G. H. Döhler, J. Phys. IV (France) **3**, 195 (1993).

[3] D. M. Whittaker, Europhys. Lett. **31**, 55 (1995).

[4] T. Meier, F. Rossi, P. Thomas, S. W. Koch, P.E. Selbmann, and E. Molinari, Phys. Rev. Lett. **75**, 2558 (1995).

[5] F. Rossi, T. Meier, P. Thomas, and S. W. Koch, Phys. Rev. **B 51**, 16 943 (1995).

[6] S. Schmitt-Rink, D.S. Chemla, and H. Haug, Phys. Rev. B **37**, 941 (1988).

[7] M. Lindberg and S.W. Koch, Phys. Rev. B **38**, 3342 (1988).

[8] H. Haug and S.W. Koch, *Quantum Theory of the Optical and Electronic Properties of Semiconductors*, 3rd ed. (World Scientific, Singapore, 1994).

[9] D. B. Tran Thoai and H. Haug, Phys. Rev. **B 47**, 3574 (1993).

[10] J. Schilp, T. Kuhn, and G. Mahler, Phys. Rev. **B 50**, 5435 (1994).

[11] For a review see F. Rossi, R. Brunetti, and C. Jacobini, in *Hot Carriers in Semiconductor Nanostructures: Physics and Applications*, edited by J. Shah (Academic Press, Boston, 1992), p. 153.

[12] R. Brunetti, C. Jacoboni, and F. Rossi, Phys. Rev. **B 39**, 10 781 (1989).

[13] L. Esaki, and R. Tsu, IBM J. Res. Dev. **14**, 61 (1970).

[14] A. Stahl, Z. Phys. B **72**, 371 (1988).

[15] I. Balslev, R. Zimmermann, and A. Stahl, Phys. Rev. **B 40**, 4095 (1989).

[16] E. Molinari, in *Confined Electrons and Photons: New Physics and Applications*, edited by E. Burstein and C. Weisbuch (Plenum, New York, 1994).

[17] H. Rücker, E. Molinari, and P. Lugli, Phys. Rev. B **45**, 6747 (1992).

[18] For a review see A. Stahl, I. Balslev, *Electrodynamics of the Semiconductor Band Edge*, Springer Tracts in Modern Physics Vol. 110 (Springer, Berlin, 1987).

[19] G. Bastard, *Wave Mechanics Applied to Semiconductor Heterostructures* (Les Editions de Physique, Les Ulis, France, 1988).

[20] P. Leisching, P. Haring Bolivar, W. Beck, Y. Dhaibi, F. Brüggemann, R. Schwedler, H. Kurz, K. Leo, and K. Köhler, Phys. Rev. B **50**, 14 389 (1994).

[21] K. H. Schmidt, N. Linder, G. H. Döhler, H. T. Grahn, K. Ploog, and H. Schneider, Phys. Rev. Lett. **72**, 2769 (1994).

[22] M. M. Dignam and J. E. Sipe, Phys. Rev. B **43**, 4097 (1991).

[23] R. Zimmermann, Phys. Status Solidi B **159**, 317 (1990).

[24] A. V. Kuznetsov, Phys. Rev B **44**, 13381 (1991)

[25] R. Brunetti, C. Jacoboni, and F. Rossi, Phys. Rev. B **39**, 10 781 (1989).

[26] P. Lipavsky, F. S. Khan, A. Kalvova, and J. W. Wilkins, Phys. Rev. B **43**, 6650 (1991).